

Contents lists available at ScienceDirect

Composites Part B

journal homepage: www.elsevier.com/locate/compositesb





A sustainable manufacturing method of thermoset composites based on covalent adaptable network polymers

Xu He^a, Xiaojuan Shi^{a,b}, Christopher Chung^a, Zepeng Lei^c, Wei Zhang^c, Kai Yu^{a,*}

- ^a Department of Mechanical Engineering, University of Colorado Denver, Denver, CO, 80217, USA
- b National Key Laboratory of Science and Technology on Advanced Composites in Special Environments, Harbin Institute of Technology, Harbin, 150080, PR China
- ^c Department of Chemistry, University of Colorado Boulder, Boulder, CO, 80309, USA

ARTICLE INFO

Keywords: Covalent adaptable network polymers Composite manufacturing Recycling Sustainability

ABSTRACT

Sustainable manufacturing of polymer composites has received increasing global attention. Existing industrial manufacturing methods rapidly consume natural resources and generate significant manufacturing wastes that are difficult to recycle. In this study, we develop a sustainable manufacturing method for thermoset composites based on the dynamic features of covalent adaptable network (CAN) polymers. It uses the scrap polymer wastes as feedstock to fabricate solid polymer films with tailored thicknesses. They are used to manufacture composite lamina with controlled fiber contents *via* hot pressing, wherein the malleable matrix fuses into the fiber fabric and welds them together. Both fiber and thermoset matrix can be recycled for the next round of manufacturing. The composites exhibit near-identical mechanical performance in each manufacturing cycle as the ones directly molded with the polymer solution. The fabricated composites are malleable and can be readily reprocessed into different shapes without using complicated molding tools. Compared to the conventional manufacturing methods, the developed one significantly decreases the consumption of nonrenewable resources, polymer waste generation, as well as manufacturing cost. It has the great potential to be applied to a wide variety of polymer systems.

1. Introduction

Fiber-reinforced polymer composites have been leading contenders of load-bearing structural materials due to their superior combination of high stiffness, high strength, and lightweight [1,2]. When employing cross-linking thermosets as the matrix, the composites exhibit enhanced thermal stability, chemical resistance, and structural integrity, which enable their high-performance applications in aerospace, automotive, renewable energy, and athletic industries [3,4].

In recent years, sustainable development has received increasing global attention from both the public and business sectors. The Environmental Protection Agency defines sustainable manufacturing as "the creation of manufactured products through economically-sound processes that minimize negative environmental impact while conserving energy and natural resources [5]." However, most industrial manufacturing methods of thermoset composites do not fully comply with this definition. They rapidly deplete finite natural resources because most synthetic polymers and fibers are derived from non-renewable petroleum. The significant wastes generated during the manufacturing process are difficult to

recycle and are eventually released into the environment or in landfills, leading to considerable economic loss and environmental burden [6–8]. Additionally, the feedstock materials for composite manufacturing generally have a limited shelf life depending on the storage conditions (e.g., temperature, oxygen, light irradiation). For example, using a prepreg has been a commonly used method for on-site manufacturing of composites [9,10], which has a shelf life of only three to twelve months at room temperature [11–13]. Therefore, the prepregs must be frozen and stored before use. Recycling expired prepregs is challenging and may lead to additional waste. Furthermore, conventional manufacturing methods for composites, including vacuum bagging, resin transfer molding, filament winding, and pultrusion [14–17], all require expensive molding tools to shape the resin and fiber. Once the matrix is cured, the composites cannot be reprocessed and reshaped.

By leveraging the recently developed covalent adaptable network (CAN) polymers [18–26], fundamental challenges of composite manufacturing in sustainable development can be tackled. CANs are cross-linked networks with mechanical performance comparable to conventional thermosets, but the dynamic nature of reversible bonds

E-mail address: kai.2.yu@ucdenver.edu (K. Yu).

^{*} Corresponding author.

allows them to rearrange the network topology through bond exchange reactions (BERs) when a stimulus is given (e.g., heat) [27-31]. The dynamic networks exhibit exciting features that are not seen in conventional thermosets. First, the chain cleavage during a BER releases the internal stress, so the network is malleable and can be reprocessed into different shapes or functionalities [18,19,23,32-39]. Second, When CANs are brought into contact, polymer chains connect on the interface through BERs. This interfacial welding enables the damaged thermosets to be fully repaired [40-45]. Third, primary recycling of the dynamic networks can be realized using a solution of small organic molecules with mild processing conditions [46-56]. The small molecules diffuse into the network and depolymerize the CANs by breaking dynamic bonds on the chain backbone. Re-polymerization occurs via heating to evaporate the solvent and small molecule byproduct. The recycled polymers exhibit near-identical network structure and mechanical properties as unprocessed ones.

In this paper, we develop a sustainable manufacturing method for thermoset composites based on the dynamic features of polyimine-based CANs [57]. Polyimine thin films are first fabricated by recycling composite scraps, which are used as feedstock for composite manufacturing. A composite lamina can be fabricated by sandwiching a carbon fiber fabric between two polyimine films under the hot-pressing condition. The fabricated lamina is malleable and can be reprocessed into different shapes depending on applications. It can also be assembled into laminate structures by leveraging the interfacial welding effect of the polyimine matrix. Finally, the fabricated composites can be recycled by depolymerizing the CAN matrix. The reclaimed fiber fabric and thermoset resin are available for the next round of manufacturing.

One of the major novelties of the developed method is that a fully cured thin-film thermoset, which is recycled from composite scraps, is used as feedstock for composite manufacturing. Due to the dynamic chemistry, the solid polymeric materials can fuse into the fiber fabric in the microscale and weld them together into a robust composite sample. Compared to the prepreg, the storage of feedstock polyimine is much easier, and its usage is safer during the on-site composite manufacturing. The feedstock shelf life could be greatly extended if they are stored in an appropriate condition, such as avoiding moisture and elevated temperature. The fabricated composites can be readily reprocessed into different shapes via simple heating, thus avoiding expensive molding tools during the on-site manufacturing of composite components. To demonstrate the great application potential of the manufacturing method, we use a polyimine-based CAN as the model system, which has low processing temperature and catalyst-free features. But the newly developed manufacturing method reported herein can be readily extended to other CAN systems and is scalable for practical industrial applications.

2. Material and methods

2.1. Synthesis of polyimine CANs and their solvent-assisted recycling

The polyimine-based CAN was synthesized following the previous work of Philip et al. [57]. It was prepared from linear monomer terephthaldehyde (dialdehyde), diethylene triamine (diamine), and the cross-linker tris(2-aminoethyl) amine (triamine) (Fig. 1). The

Fig. 1. Preparation of the polyimine CANs using dialdehyde, diamine monomers, and triamine cross-linker. The dynamic C—N bond on the chain backbone is highlighted.

terephthaldehyde and diethylene triamine were purchased from Sigma-Aldrich (St. Louis, MO, USA), and the tris(2-aminoethyl) amine was purchased from Alfa Aesar (Haverhill, MA, USA).

The schematic view of the polymerization process is shown in Fig. 1. Polyimine film was synthesized from a mixture of terephthaldehyde (TPA), diethylene triamine (DETA) and tris(2-aminoethyl)amine (TREN) at a molar ratio of 1.00 : 0.30: 0.47. TPA (4.44 g, 33.1 mmol) and DETA (1.02 g, 9.90 mmol) were dissolved in ethanol (80 mL). After the mixture became homogeneous, a solution of TREN (2.26 g, 15.4 mmol) in 20 mL of ethanol was added, and the solution was transferred to a box-shaped tray (10 cm \times 10 cm \times 2 cm) made from a siliconecoated release paper. The solvent was then allowed to evaporate in a fume hood under ambient conditions to form a polymer film. The resulting film was further cured by the hot pressing at 75 °C for 2 h, then at 85 °C for 2 h, and, finally, at 105 °C for 2 h. The synthesized polyimine CANs exhibit a glass transition temperature (T_g) around 75 °C, which allows for their applications as structural load-bearing materials at room temperature. For the dry polyimine sample, the network with dynamic C=N bonds on the chain backbone (highlighted in Fig. 1) can go through imine exchange reactions at temperatures above ~80 °C, which enable the network malleability and interfacial welding effect.

Primary recycling of the polyimine CAN can be enabled using an amine-based solvent. As shown in Fig. 2, when the polyimine is soaked in propylamine (Sigma Aldrich, without purification) at elevated temperatures (e.g., 50–90 °C), the amine molecules diffuse into the network and participate in imine exchange reactions with the dynamic C=N groups on the chain backbone. Since the small amine molecules are not linked to the long polymer chains, they effectively break the polymer chains into short-chain segments and eventually depolymerize the network into soluble oligomers. Such a process is reversible, and repolymerization occurs when the solution is heated to remove the propylamine, driving the equilibrium toward the CAN formation.

2.2. Overview of the sustainable manufacturing process

Fig. 3 illustrates the overall manufacturing process of the carbon fiber-reinforced polyimine composites, which consists of four major steps, namely i) the preparation of polyimine thin films, ii) the preparation of polyimine composite lamina and laminate, iii) the reshaping of composite structures based on applications, and iv) the recycling of composites using propylamine solvent.

The polyimine composite scraps were first immersed in the propylamine solvent (Fig. 3a) and heated to depolymerize the matrix and reclaim the fiber (Fig. 3b). The obtained polymer solution was heated again for the re-polymerization (Fig. 3c). To facilitate the solvent

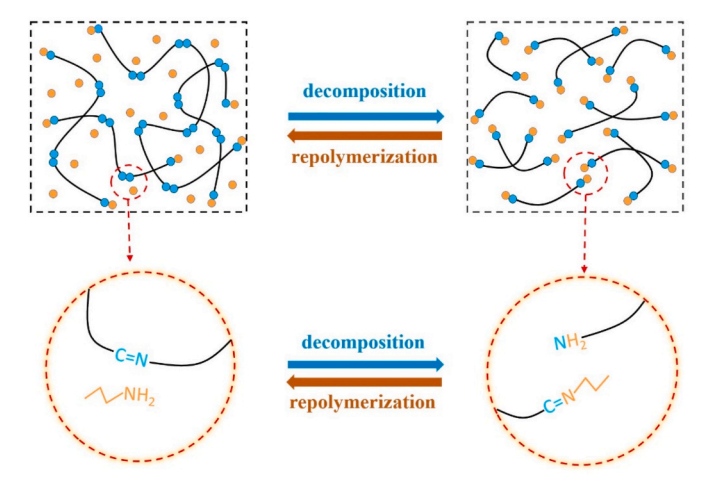


Fig. 2. Schematic views of the recycling mechanism of polyimine using propylamine solvent.

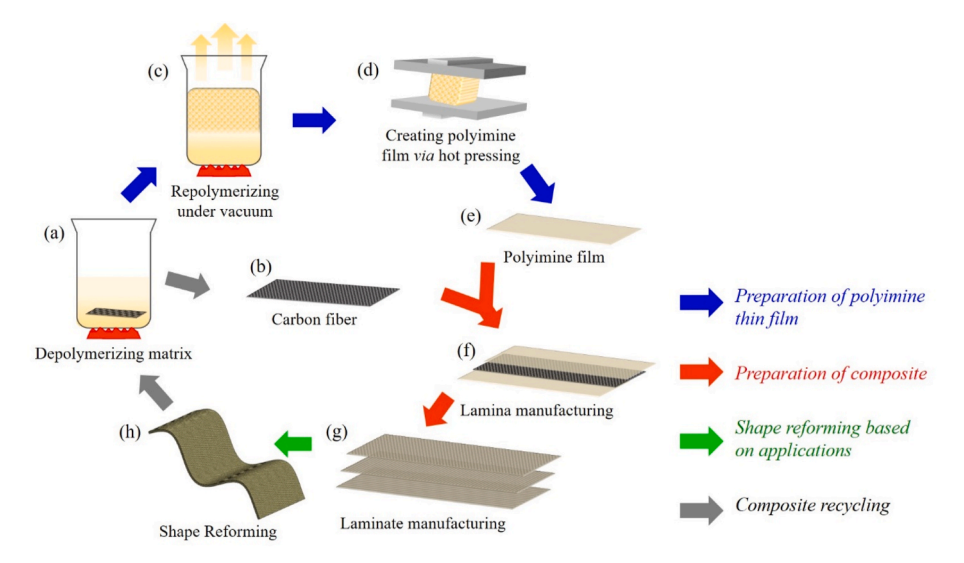


Fig. 3. Schematic presentation of the manufacturing process for polymine composites. (a) Immersing the composite scraps in solvent to depolymerize the matrix. (b) Reclaiming carbon fiber. (c) Re-polymerizing the matrix. (d) Hot pressing the foam to obtain a (e) polymine film. (f) Preparing the lamina. (g) Preparing the laminate. (h) Reshaping the composite.

evaporation, high temperature and vacuum were applied, which generated intensive bubbles during the solvent evaporation, leading to a porous polyimine after re-polymerization. To prepare the polyimine thin film, the foam was compressed at a temperature above the BER activation temperature of polyimine (Fig. 3d), which gradually closed the internal voids, and the foam was transformed into a solid thin film (Fig. 3e).

To fabricate the composite lamina, the reclaimed fiber fabric was sandwiched between two polyimine films and compressed at high temperature (Fig. 3f) until the fiber and matrix fused together. The composite laminates were fabricated by welding different layers of the lamina (Fig. 3g). Since the polyimine matrix is malleable at a high, the fabricated composite can be reshaped into different shapes according to specific applications (Fig. 3h). Finally, the manufactured composites were immersed in propylamine solvent to depolymerize the matrix and reclaim the fiber. The recycled resin and fiber were used for the next round of composite manufacturing.

2.3. Property characterization on the manufactured polyimine and composites

In this study, we focus on the manufacturing process of polyimine composites. Steps 1-3 in the above-mentioned process were experimentally characterized in different manufacturing cycles. The experimental characterizations are briefly described below. The detailed procedures are included in the Supplementary Materials (Section S1).

2.3.1. Characterizations on the recycled polyimine

Fourier-transform infrared spectroscopy (FTIR) measurements were conducted to determine if there was excessive propylamine solvent left in the re-polymerized network. Polyimine thin film was prepared by repolymerizing the depolymerization solution at 120 $^{\circ}\text{C}$ for different times. The amine group in propylamine has a unique absorption peak at 3400-3250 cm^{-1} . It was used as an indicator to evaluate the network structure of recycled polyimine, which was compared with the unprocessed networks without propylamine.

Thermomechanical properties of the recycled polyimine were characterized. The glass transition behaviors (e.g., storage modulus and network T_g) of the polyimine and their recycled samples were studied using the dynamic mechanical analysis (DMA, Model Q800, TA Instruments, New Castle, DE). Uniaxial tension tests were performed to examine their modulus and ultimate tensile strength at room

temperature. The BER-induced stress relaxation behaviors at different temperatures were characterized using the DMA tester in tension state.

2.3.2. Characterizations on the fabricated composite laminate

Fusion of the polyimine matrix with the fiber fabric during the lamina fabrication was observed using an optical microscope. The composite laminate was fabricated by welding three layers of lamina at different temperatures and pressures. The control sample was fabricated using the conventional molding process, wherein the fiber fabric was fixed in a mold. The decomposed polymer solution was poured into the mold, followed by heating to cure the resin. The control samples had the same geometry and fiber volume content as the ones fabricated based on the lamina welding. They are denoted as "directly molded samples" for the rest of the paper. All the fabricated composite laminates were subjected to three-point bending tests at room temperature to examine the structural stiffness and flexural strength.

To examine the reshaping capability, the fabricated composite lamina with different fiber volume fractions was compressed between a wave-shaped mold at different temperatures and nominal pressure. After being processed for different times, the sample was taken out and stabilized at 80 $^{\circ}\text{C}$ in a free-standing state for 30 mins. The shape fixity was determined by comparing the new shape of the lamina sample with that of unprocessed ones.

3. Results and discussions

3.1. The overall manufacturing process

The appearances of polyimine thermosets and their composites during the manufacturing process are shown in Fig. 4. Specifically, the composites are embedded with the woven carbon fiber fabric (3K, 2×2 twill weave, Fibre Glast Developments CORP., Brookville, OH, USA). The composite scraps were first immersed in the propylamine solvent (Fig. 4a) to depolymerize the matrix material and reclaim the fiber fabric (Fig. 4b). The depolymerization process was in a surface-corrosion manner. Its speed depended on the temperature, size, and surface area of scrap materials. For example, at 90 °C, a \sim 1 cm³ cubic sample was fully depolymerized within \sim 15 min.

After the polyimine matrix was fully depolymerized into a transparent yellow liquid, the polymer solution was heated at 90 $^{\circ}$ C to repolymerize the network, which was above the boiling point of the propylamine (48 $^{\circ}$ C). Note that the solvent vapor can be collected for the

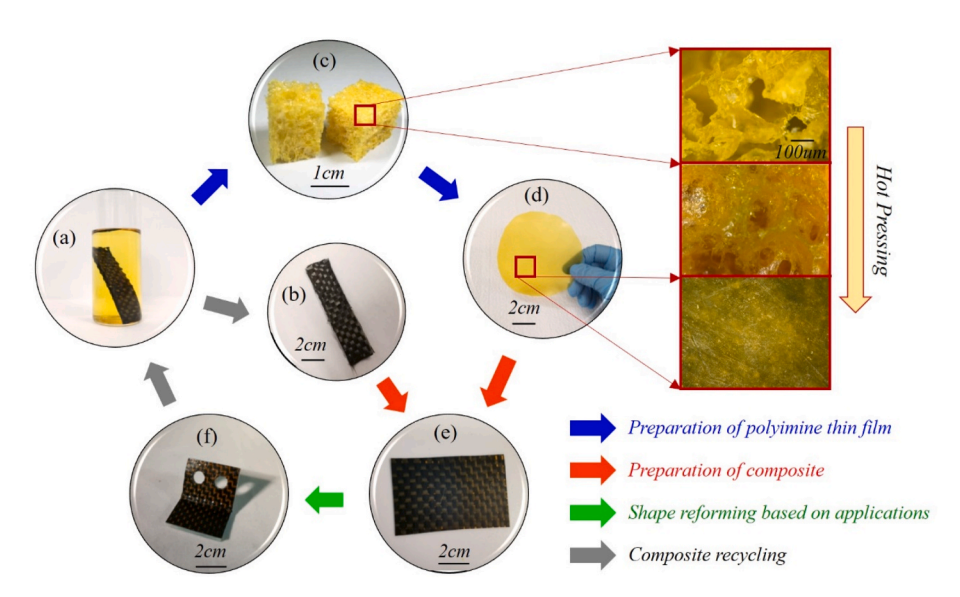


Fig. 4. Photo images of the polyimine thermosets and their composites during the manufacturing process. (a) A polyimine composite is immersed in the propylamine solvent. (b) The reclaimed carbon fiber fabric. (c) The created polyimine foam. (d) The polyimine thin film after hot pressing. (e) The prepared composite lamina. (f) The reshaped composite based on the reshaping ability of the matrix material. Inset pictures show the microscale morphology of the polyimine foam during the hot pressing.

next round of manufacturing, so there could be negligible hazardous vapor released into the environment. During the re-polymerization, the short-chain segments reconnected *via* BERs to form a cross-linking network. Without a vacuum condition, the solution would take a few hours to be fully polymerized into a solid at 90 °C. When a vacuum of 8 kPa was applied, the solvent evaporation was substantially sped up, and the re-polymerization process only took a few minutes. Consequently, significant bubbles were generated during the heating, leading to a porous polyimine material (Fig. 4c). Based on the density of the foam, its porosity was estimated to be 72%.

The polyimine foam was then subject to hot pressing at a temperature above the BER activation temperature (e.g., $120\,^{\circ}\text{C}$) with pressure applied (e.g., 1 MPa). The inset views of Fig. 4 show the morphology of internal voids observed using an optical microscope, which is shown to gradually close due to the malleability of polyimine. The foam eventually transformed into a dense solid film without any void (Fig. 4d). The thickness of the obtained polyimine film can be tailored by controlling the heating temperature, pressure, and time, which provide a reliable approach to control the quality and geometry of polyimine film fabrication. For example, after compressing at $120\,^{\circ}\text{C}$ and 1 MPa for 10 min, the film thickness was $\sim\!200\mu\text{m}$. When the compressing time was increased to 30 min, a film with $\sim\!25\mu\text{m}$ thickness was obtained.

The solid polyimine films are used as feedstock to fabricate the composite lamina. In the previous work by Yu et al. [53], the CAN composite was directly fabricated using the depolymerization solution. Here, utilizing solid thin films has two main advantages. First, the customers do not have to deal with hazardous chemicals or solvents, making the feedstocks safe to use on-site. Second, it avoids intensive solvent evaporation and volume contraction during manufacturing, which is the primary reason for the stress concentrations in conventional composite manufacturing methods. Fig. 4e shows the appearance of the fabricated composite laminate with 3 lamina layers, as well as its new geometry after reshaping (Fig. 4f). Finally, the composite was immersed in the propylamine solvent, wherein the composite matrix was depolymerized, and pristine fiber was reclaimed. Since the heating temperature was much lower than the thermal degradation temperature of carbon fiber, and the solvent did not react with it, the reclaimed fiber fabric was damage-free and could be used repeatedly for further manufacturing.

In this study, polyimine is used as the matrix material for sustainable composite manufacturing. Even though it is not a widely used engineering material in the industry or agriculture, the developed manufacturing method can be extended to other engineering thermosets. For example, in the previous studies [52,58,59], the anhydride-cured epoxy networks were shown to be recycled using an

alcohol solvent mixed with a BER catalyst, wherein both the solvent molecules and catalyst diffused into the network, broke the polymer chains from the ester bonds *via* transesterification BERs, and eventually depolymerized the network. Such ester-containing thermoset networks (others like polyester, vinyl ester, and polyurethane) are commonly used in the industry. More importantly, after re-polymerization, the BER catalyst and some hydroxyl groups were left in the network, which endowed the BER capability of the recycled materials, so they can be used as feedstock for composite manufacturing. Therefore, the developed manufacturing method has the potential to be applied in the future to use real engineering scrap materials as resources and significantly decreases the consumption of nonrenewable resources.

3.2. Step 1: properties of the prepared polyimine thin film

The properties of prepared polyimine thin film were examined, including the network structure, transition behaviors, and thermomechanical properties. Following the above-mentioned procedure, the polyimine foams were first prepared by heating the depolymerization solution at 120 °C under a vacuum level of 8 kPa. The heating time varied from 5 min to 30 min, followed by hot pressing into thin films. The FTIR trace of the recycled polyimine with 30 min of hot-pressing is shown in Fig. 5a (red dash line) and compared with that of the unprocessed network (black solid line). It is shown that the recycled polyimine exhibits similar absorption peaks to those of the original one over the entire range of the spectrum, such as the dynamic C=N on the chain backbone at 1660 cm⁻¹, the C-N stretch of the secondary amine at 1214 cm⁻¹, and the C-N stretch of the tertiary amine at 1143 cm⁻¹.

The N–H stretch of primary amines, which belongs to the propylamine solvent used for the recycling, shows peaks in the region from $3400~{\rm cm}^{-1}$ to $3250~{\rm cm}^{-1}$ and is highlighted in Fig. 5b. For primary amines, there are two absorption peaks in this region, which respectively correspond to the asymmetrical N–H stretch and the symmetrical N–H stretch. It is observed that the peak height decreases with the heating time. This suggests that the generated propylamine molecules are gradually evaporated out of the system. After being heated at $120~{\rm ^{\circ}C}$ for 30 min, the content of primary amine reaches almost the same level as that of a fresh sample, suggesting that the network microstructure is fully restored in the re-polymerized polyimine.

The depolymerization and re-polymerization cycle of polyimine thin films was repeated multiple times. The samples were then subject to the DMA measurements. The evolutions of storage modulus and $\tan\delta$ during the glass transition process are shown in Fig. 6a. Even after being recycled four times, the polyimine network still maintains the same level

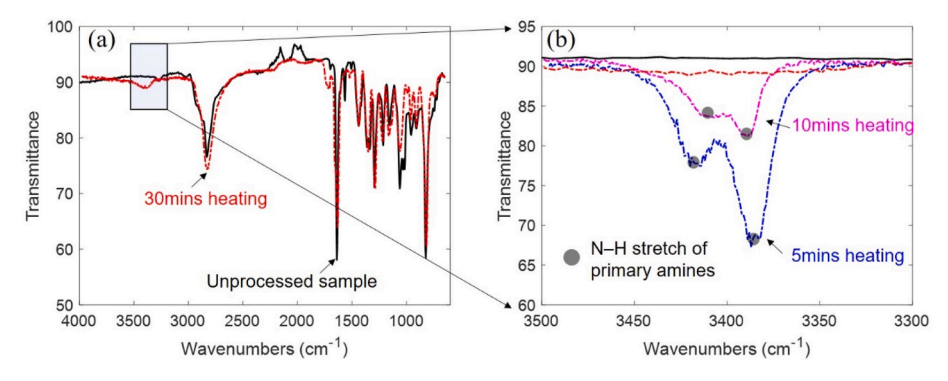


Fig. 5. (a) FTIR results of the fresh polyimine and polyimine after re-polymerization. (b) Zoom-in view of the absorption peaks of primary amines with different heating times during the preparation of polyimine thin film.

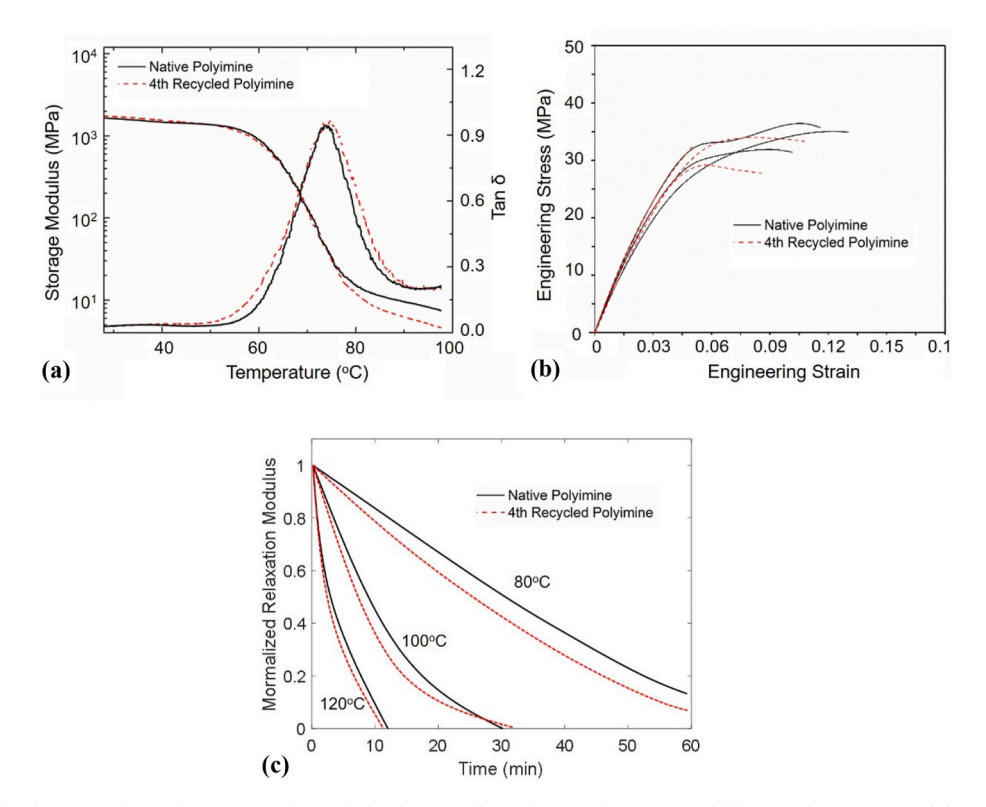


Fig. 6. Comparison of the thermomechanical properties of recycled polyimine film and original unprocessed film. (a) The storage modulus and $\tan \delta$ during the glass transition. (b) The room-temperature stress-strain relationship. (c) BER-induced stress relaxation at different temperatures.

of network T_g and modulus over the testing temperature range. The room-temperature strain-stress relationships are compared in Fig. 6b. The recycled network also exhibits similar Young's modulus and mechanical strength compared to the original one. At a high temperature, the active BERs induce stress relaxation. The normalized relaxation modulus of fresh and recycled polyimine are shown in Fig. 6c. A higher temperature leads to a faster drop in internal stress. At 120 °C, the stress is seen to be fully released in ~10 min s. The close comparison in Fig. 6c shows near-identical relaxation behaviors of the recycled sample. Overall, the mechanical characterizations confirm that the network macroscale thermomechanical properties are recovered in the repolymerized polyimine.

3.3. Step 2: fabrication of composite lamina and laminate

3.3.1. Fusion of polyimine matrix with the fiber fabric

The composite lamina was fabricated by sandwiching a woven fiber fabric (\sim 0.55 mm thickness) between two polyimine thin films and then

subjecting them to the hot pressing. The malleable polyimine is expected to fully permeate through the fiber bundle after processing, which removes any voidbetween the fiber and polymer matrix, thus improving the quality and mechanical performance of the fabricated composites.

The microscopic morphology of the composite lamina was examined using an optical microscope. To prepare the lamina sample, polyimine films with a thickness of ${\sim}620\mu m$ were used. Based on the density and weight of the polymer matrix and fiber fabric, the fiber volume fraction of the fabricated lamina is ${\sim}30.7\%.$ To select a suitable pressure for the hot pressing, one may need to consider both the modulus and strength of dynamic polymers. When the BERs are activated within the network, the materials essentially behave like viscous liquids, so a higher pressure (e. g., comparable to the network modulus) could substantially promote the fusion of the material. On the other hand, excessively high pressures above the material strength will lead to the fracture of the material on the macro- or micro-scale during the processing. While the network welding effect can help close the voids, it will lower the processing efficiency, and the extent of repair is unknown.Based on these

considerations, the temperature was set to be 80 °C and a 1 MPa pressure was applied as the starting point during the hot pressing. Fig. 7a shows the side view of a fiber bundle within the composite lamina after being heated for different times. It is observed that after 1 h of heating, the fiber bundle and matrix can be distinguished under an optical microscope, while after 6 h, they are fused together without a clear boundary. The optical microscope observations on the side appearance and the cross-sectional view of the fiber bounder in the lamina after 6 h of heating are shown in Fig. 7b. They confirm that the polyimine has fully permeated into the fiber bundle and fused together after the hot pressing. There are no notable defect or void in the microscale around the fiber and matrix interfaces. It should be noted that during the hot pressing of the lamina, the in-plane flow of the polyimine matrix was observed to be suppressed, which could be a result of the confinement of the fiber fabric. Therefore, the fiber volume fraction does not change significantly over time.

In addition to the microscale observations, lap-shear tests were performed to examine the mechanical bonding strength between the fiber fabric and the polyimine matrix. The samples were prepared by sandwiching a woven fiber fabric between two polyimine films in the overlapping area, wherein the fiber content was tailored using polymer film with different thicknesses. After being heated for a given time under pressure, the welded sample was stretched in the length direction. A control lap-shear sample was directly molded with the same fiber content. The testing results are shown in the Supplementary Materials (Section S2). It is observed that with a sufficient heating time, the ultimate bonding strength of samples with relatively low fiber content eventually reaches the same level as the control sample. Increasing temperature dramatically speeds up the welding process. Pressure is also seen to be a positive parameter to promote the bonding strength due to the enhanced viscous flow and fusion of the matrix [60–63].

However, when the fiber content is higher than \sim 49.4%, the ultimate shear strength starts to decrease. To understand the reason, we examined the microscale morphology of the fiber-matrix interfaces of the sample with \sim 55% fiber content. The sample was manually cut over the welding region. Fig. S2 shows the cross-sectional view. We can observe that after welding at 120 °C for 6 h, the matrix materials can fuse inside the fiber fabric to weld individual fibers, but there are considerable defects and voids among the bonded fiber aggregates. Compared to the conventional composite manufacturing methods that using liquid precursors, the one presented in this work leverages the solid-plasticity of polyimine materials, which may not be able to provide a good fiber surface wetting when the fiber content is above a critical value. How to overcome this drawback to enable a high fiber content

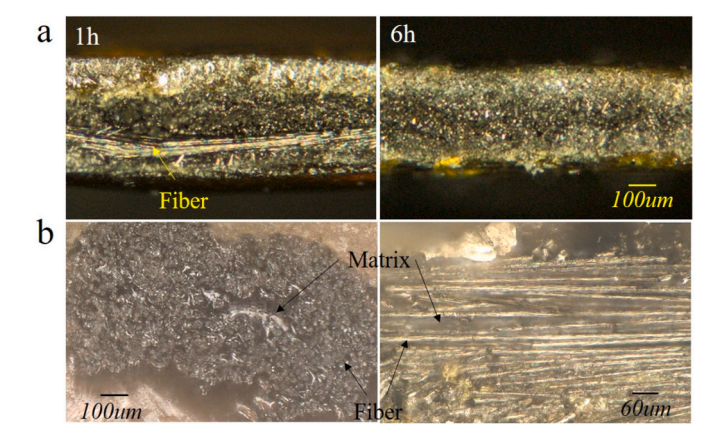


Fig. 7. Microscopic images to show the fusion between the polyimine matrix and carbon fiber. (a) Optical microscope observations on a fiber bundle within the composite lamina after being heated for 1 h and 6 h. (b) The optical microscope observation on the lamina side appearance and the cross-sectional view of the fiber bounder after being heated for 6 h.

deserves further study.

3.3.2. Structural stiffness and strength of composite laminate

Based on the above experimental results, four types of lamina samples were parepared with different fiber contents below the critical value (30.7%, 39.6%, 44.1%, and 49.4%). The corresponding thicknesses of the polyimine film are listed in Table 1. All the samples were welded at $120\,^{\circ}$ C for 6 h with 3 MPa pressure applied.

The composite lamina was used to fabricate laminate structures, which relied on the interfacial welding effect of the polyimine matrix. Lap-shear tests were first performed to examining the bonding strength between lamina samples with different fiber contents. The testing results are shown in the Supplementary Materials (Section S3). It is observed that the ultimate shear strength increases with time and temperature as more polymer chains are connected on the interface *via* BERs [64–67]. The strength can eventually reach ~17.7 MPa, which is almost the same level as the directly molded sample. On the other hand, for the lamina samples with higher fiber content, the amount of polyimine material on the sample surfaces, which is responsible for the interfacial welding between the composite lamina, will be dramatically decreased. The samples also exhibit a higher level of surface roughness. Therefore, they require a higher welding pressure (3 MPa) to enable a bonding strength that is comparable to the directly molded sample.

Three-point bending tests were performed to evaluate the structural stiffness and strength of the welded composite laminate. Based on the study shown in Fig. S3, the Lamina 4 sample with 49.4% fiber content was used as the material platform. Three pieces of the lamina with the same dimension (10 mm \times 80 mm \times 0.23 mm) were first welded at 120 °C with 3 MPa pressure applied. After welding for a given time, the laminate samples were subject to three-point bending tests on the MTS machine. Since the sample thickness was 0.69 mm, the span length was set to 38 mm to achieve the 60:1 support span-to-thickness ratio (per ASTM standard D7264). During the tests, the crosshead moving rate was set to 1 mm/min, and the test ran until a crosshead extension of 15 mm was completed. The force (*P*) - displacement (δ) relation was recorded. The flexural stress at the outer surface mid-span was calculated as $\sigma =$ $3PL/2bh^2$, with L being the support span length, b being the support span length, and h being the sample thickness. The strain at the outer surface was calculated using $\varepsilon = 6\delta h/L^2$. After testing, the matrix and fiber fabric of the composite samples were recycled using propylamine solvent and used to fabricate a new piece of sample with the same fiber content. The welding and three-point bending tests were repeated with identical processing conditions.

Fig. 8a shows the relationship between flexural stress and flexural strain of the laminate sample with different welding times. The experimental data of the directly molded control sample with the same fiber content is also plotted for comparison. With the increment of welding time, the interfacial bonding strength between adjacent lamina increases, leading to an enhanced flexural strength of the laminate sample. After being welded for $\sim\!30$ min, the flexural strength reaches the same level as the control sample. It is also prominent to observe that after being recycled four times, the laminate samples exhibit similar mechanical performance compared to the first-generate manufactured sample, suggesting good recyclability and repeatability of the polyimine matrix for composite manufacturing.

The structural flexural stiffness and flexural strength of the composite laminate are summarized as a function of welding time at 120 $^{\circ}\text{C}$

Table 1Thickness of polyimine film and the fiber content of lamina samples.

	Thickness of polyimine film	Fiber volume fraction
Lamina 1	620 μm	30.7%
Lamina 2	420 μm	39.6%
Lamina 3	350 μm	44.1%
Lamina 4	276 μm	49.4%

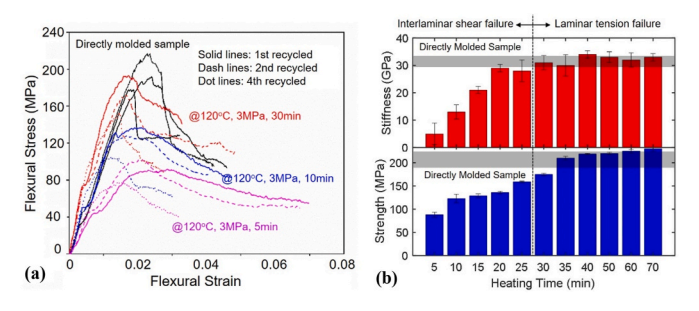


Fig. 8. (a) The relationship between flexural stress and flexural strain with different welding time. (b) Summary of the structural stiffness and flexural strength as a function of welding time at 120 $^{\circ}$ C.

in Fig. 8b. Specifically, the structural flexural stiffness was calculated by determining the initial slope of the stress-strain curve in Fig. 8a below 0.3% strain. Overall, at the early stage of heating, the structural flexural stiffness and flexural strength increase almost linearly with processing time. The stiffness is observed to first reach the level as the directly molded sample (in $\sim\!20$ min), while the strength increment takes $\sim\!35$ min s to saturate. The failure modes of the laminate samples with different welding times are marked in the figure. Due to the gradually enhanced interfacial strength, the failure model translates from interlaminar shear failure to laminar tension failure after being welded for $\sim\!25 \mathrm{min}$.

3.4. Step 3: reshaping of polyimine and their composites

An effective reshaping capability of thermoset composites will enable the rapid onsite manufacturing of composite products without using expensive molding tools, leading to a manufacturing process that is both economical and sustainable. While the previous studies show that a CAN sample can permanently fix the reprocessed shape after releasing the internal stress, the reshaping capability of their composites remains unclear and deserves investigation, especially when the stiff fiber fabric tends to recover the original flat geometry.

Polyimine thin film and composite lamina with different fiber contents were subjected to the reshaping tests using a sine-wave mold with a wavelength of 50 mm (Fig. 9a) to examine the reprocessing capabilities. The samples were cut into the same width (10 mm) and length (80 mm). During the tests, the samples were first heated at a specific temperature above the BER activation temperature for different times and then placed in the mold with a force applied on the top. The average reprocessing pressure was taken to be the force divided by the nominal area. After being heated for a given time, the sample was taken out and allowed for stabilization at the same temperature for 5 min before measuring the average wavelength.

Fig. 9a shows the appearance of the polyimine film and the Lamina 4 sample with 49.4% fiber after being reprocessed at 120 °C for different times. The nominal reprocessing pressure was 3 MPa for each case. It is observed that the average sample wavelength gradually decreases towards the target number of the mold ($\lambda_t = 50$ mm). The reprocessing of polyimine film is more efficient, wherein the new shape can be completely fixed after being heated for ~20 min, while the complete

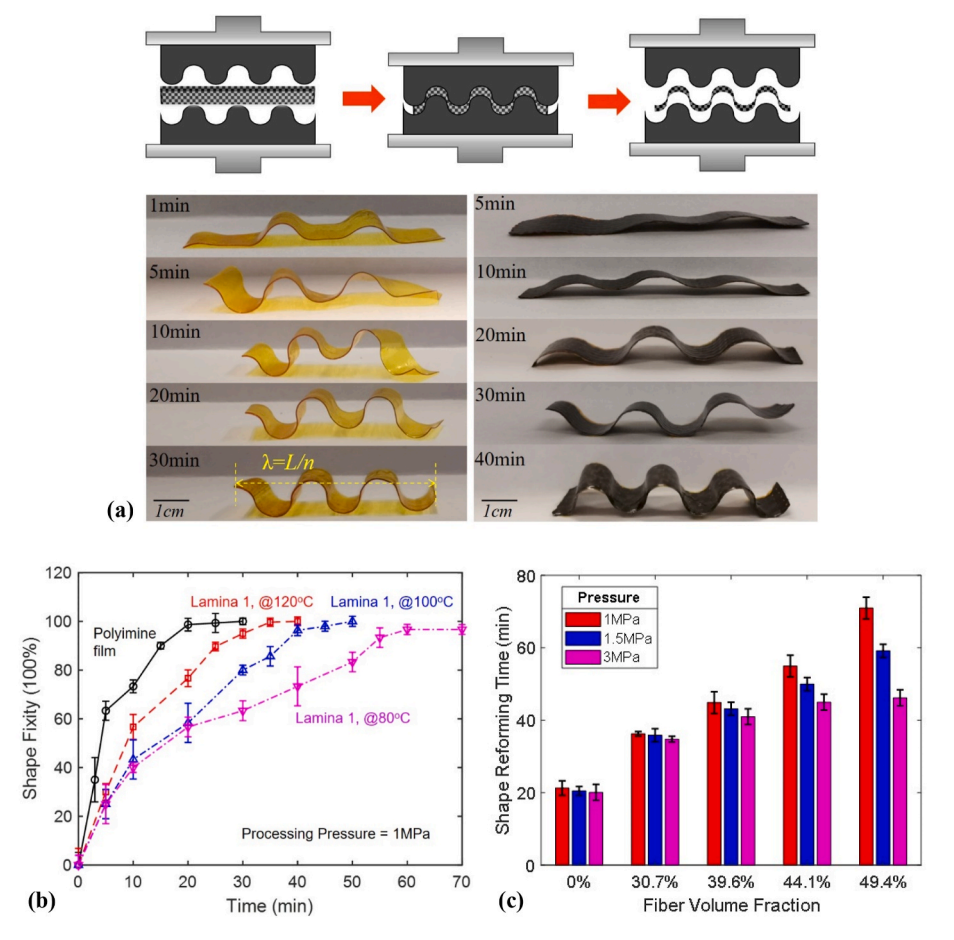


Fig. 9. (a) Schematic views of the experimental procedure and the experimental images during the reshaping tests. The tests were conducted on pure polyimine and composite lamina samples. (b) Evolution of the shape fixity as a function of reprocessing time at different temperatures. (c) Comparison of the reshaping time of the polyimine and lamina with different fiber contents. The reprocessing temperature was set to be 120 °C for all cases.

reprocessing of the lamina sample takes ~40 min.

Based on the measured wavelength (λ), a shape fixity ratio (R_f) is defined to characterize the reshaping ability. It is calculated as $R_f = 1$ $(\lambda_0 - \lambda)/(\lambda_0 - \lambda_t)$, with λ_0 being the initial wavelength of the sample without reprocessing. According to the same length and mold geometry, $\lambda_0 = 16$ mm. The evolutions of shape fixity of the polyimine film and the lamina sample are summarized in Fig. 9b as a function of reprocessing time, wherein the temperature is 80 °C, 100 °C, and 120 °C, respectively. The results show that reprocessing efficiency of the composite lamina is lower than the pure polyimine due to the presence of fiber fabric. The shape fixity of the composite lamina increases with both temperature and reprocessing time, a phenomenon that resembles the timetemperature superposition principle of polymer viscoelasticity. It also suggests that even with a relatively low reprocessing temperature of 80 °C, the shape fixity can eventually reach ~100% after ~50 min. It should be noted that the final shape fixity after the extended heating time also depends on the curvature of the intended reprocessing geometry. At positions of sharp angles with higher curvature, the fiber fabric would provide a higher resistance force for reshaping, and the final shape fixity of the composite lamina may be lower than 100%.

The shape fixity tests were repeated on lamina samples with different fiber content and pressure level. The reprocessing temperature was set to be $120\,^{\circ}\text{C}$ for all cases. The reshaping time, namely the time point when the shape fixity reaches $\sim\!100\%$, is plotted in Fig. 9c. The pure polyimine requires the lowest amount of time ($\sim\!20\,\text{min}$ s) to be fully reprocessed into the target shapes, and the reprocessing efficiency is observed to be independent of the applied pressure. The reshaping time of composite lamina increases with the fiber content, suggesting a decreased reprocessing efficiency. In addition, the effect of reprocessing pressure tends to be more notable for the lamina with higher fiber content. When the pressure was increased from 1 MPa to 3 MPa, the reshaping time of the Lamina 4 sample was decreased from $\sim\!76\text{min}$ to $\sim\!41\text{min}$, which is comparable to that of the laminar sample with lower fiber content.

Modern composite products demand laying composite film on the 3D surface, which would enhance mechanical properties of objects, or introduce electrical and thermal functions. Based on the reshaping ability of the polyimine composite lamina, a composite film can be readily coated onto a 3D object. As demonstrations, the composite lamina with 30.7% fiber was heated using a heat gun at ~120 °C and then attached to the surfaces of 3D objects (Fig. 10), including the wings and body of an airplane, an angle bracket, and the handle of a tennis racket. After heating for another ~30 min s, the composite lamina can permanently maintain its geometry at elevated temperatures. Compared to the conventional composite manufacturing and surface coating techniques, such as prepreg, the developed method based on the CAN lamina offers unique advantages. First, it allows easy and rapid onsite manufacturing without interactions with hazardous organic solvents. Second, the storage of raw materials is much easier and safer to the users. Their shelf life could be greatly extended if they are stored in an appropriate condition, such as avoiding moisture and elevated temperature. Third, the composite can be readily reprocessed into different geometries based on applications and can be fully recycled once damaged or retired.

4. Conclusions

In this work, a sustainable manufacturing method for thermoset composites is developed based on the innovative features of covalent adaptable network (CAN) polymers, including network malleability, interfacial welding, and solvent-assisted recyclability. A composite lamina can be fabricated by sandwiching a woven fiber fabric between polyimine thin-films with tailored thickness under hot pressing. After being processed under certain conditions (e.g., 80 °C, 1 MPa for 6 h), it is shown that the macroscopic and solid polyimine materials can fully fuse into the fabric and weld them together. Their shear bonding strength is shown to be comparable to that of the directly molded control sample

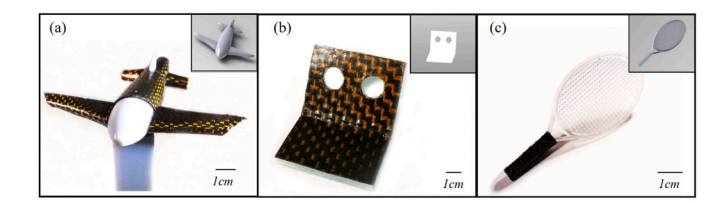


Fig. 10. Demonstration on the reshaping capability of the polyimine composites that can be mounted onto the surface of 3D objects, including (a) the wings and body of an airplane, (b) an angle bracket, and (c) the handle of a tennis racket.

with the same fiber content. The manufacturing efficiency can be further improved by increasing temperature or pressure. The approach was shown to manufacture composites with carbon fiber content up to 49.4%. Composite laminate can be fabricated by welding multiple lamina layers. After being processed at 120 °C for 35 min, both the structural flexural stiffness and flexural strength are shown to reach the same level as the control samples. Given the excellent recyclability of the polyimine CAN matrix, the manufacturing process can be repeated multiple times using the same polymer matrix and fiber fabric. The composites also exhibit excellent reshaping capability, which allows the customers to easily fabricate the composite products onsite without using expensive molding tools. Due to the booming development of dynamic covalent chemistry recently, the presented manufacturing technique can be extended to other polymer systems. It shows great potential to reduce the consumption of nonrenewable resources for composite manufacturing, minimize the hazardous wastes released to the environment, and dramatically lower the manufacturing cost, which contributes to the sustainable development of society.

Author statement

Xu He: Conceptualization, Methodology, Visualization, Writing – original draft. Xiaojuan Shi: Methodology, Investigation, Visualization, Writing – original draft. Christopher Chung: Investigation, Visualization, Writing – original draft. Zepeng Lei: Validation, Methodology, Investigation, Visualization. Wei Zhang: Validation, Methodology, Writing – review & editing. Kai Yu: Conceptualization, Writing – review & editing, Supervision, Project administration, Funding acquisition.

Declaration of competing interest

The authors declare that they have no known competing financial interests or personal relationships that could have appeared to influence the work reported in this paper.

Acknowledgment

K.Y. acknowledges support from the National Science Foundation (grant CMMI-1901807).

Appendix A. Supplementary data

Supplementary data to this article can be found online at https://doi.org/10.1016/j.compositesb.2021.109004.

References

- Sathishkumar T, Naveen Ja, Satheeshkumar S. Hybrid fiber reinforced polymer composites—a review. J Reinforc Plast Compos 2014;33(5):454–71.
- [2] Rahmani H, Najafi SHM, Ashori A. Mechanical performance of epoxy/carbon fiber laminated composites. J Reinforc Plast Compos 2014;33(8):733–40.
- [3] Tehrani M, et al. Mechanical characterization and impact damage assessment of a woven carbon fiber reinforced carbon nanotube–epoxy composite. Compos Sci Technol 2013;75:42–8.

- [4] Taraghi I, Fereidoon A, Taheri-Behrooz F. Low-velocity impact response of woven Kevlar/epoxy laminated composites reinforced with multi-walled carbon nanotubes at ambient and low temperatures. Mater Des 2014;53:152–8.
- [5] Kulatunga A, et al. Sustainable manufacturing based decision support model for product design and development process. Procedia CIRP 2015;26:87–92.
- [6] Duflou JR, et al. Environmental impact analysis of composite use in car manufacturing. CIRP annals 2009;58(1):9–12.
- [7] Sakai S-i, et al. An international comparative study of end-of-life vehicle (ELV) recycling systems. J Mater Cycles Waste Manag 2014;16(1):1–20.
- [8] Santini A, et al. End-of-Life Vehicles management: Italian material and energy recovery efficiency. Waste Manag 2011;31(3):489–94.
- [9] Davidovits J, Davidovics M. Geopolymer: ultra-high temperature tooling material for the manufacture of advanced composites. How Concept Becomes Reality 1991; 26:1020, 40
- [10] Hamerton I, Hay JN. Recent technological developments in cyanate ester resins. High Perform Polym 1998;10(2):163–74.
- [11] Jones RW, Ng Y, McClelland JF. Monitoring ambient-temperature aging of a carbon-fiber/epoxy composite prepreg with photoacoustic spectroscopy. Compos Appl Sci Manuf 2008;39(6):965–71.
- [12] Cole K, et al. Room temperature aging of Narmco 5208 carbon-epoxy prepreg. Part I: physicochemical characterization. Polym Compos 1989;10(3):150–61.
- [13] Ji K, et al. Evaluation of glass fibre/epoxy prepreg quality during storage. Polym Polym Compos 2002;10(8):599–606.
- [14] Rohatgi, V., et al., Cellulose-polymer composites and related manufacturing methods. 2003, Google Patents.
- [15] Frketic J, Dickens T, Ramakrishnan S. Automated manufacturing and processing of fiber-reinforced polymer (FRP) composites: an additive review of contemporary and modern techniques for advanced materials manufacturing. Additive Manufacturing 2017;14:69–86.
- [16] Astrom BT. Manufacturing of polymer composites. CRC press; 1997.
- [17] Papargyris D, et al. Comparison of the mechanical and physical properties of a carbon fibre epoxy composite manufactured by resin transfer moulding using conventional and microwave heating. Compos Sci Technol 2008;68(7–8):1854–61.
- [18] Scott TF, et al. Photoinduced plasticity in cross-linked polymers. Science 2005;308 (5728):1615–7.
- [19] Scott TF, Draughon RB, Bowman CN. Actuation in crosslinked polymers via photoinduced stress relaxation. Adv Mater 2006;18(16):2128–32.
- [20] Montarnal D, et al. Silica-like malleable materials from permanent organic networks. Science 2011;334(6058):965–8.
- [21] Capelot M, et al. Metal-catalyzed transesterification for healing and assembling of thermosets. J Am Chem Soc 2012;134(18):7664–7.
- inermosets. J Am Chem Soc 2012;134(18):7664–7.

 [22] Jin Y, et al. Recent advances in dynamic covalent chemistry. Chem Soc Rev 2013; 42(16):6634–54.
- [23] Taynton P, et al. Heat- or water-driven malleability in a highly recyclable covalent network polymer. Adv Mater 2014;26(23):3938-42.
- [24] Ponnuswamy N, et al. Discovery of an organic trefoil knot. Science 2012;338 (6108):783-5.
- [25] Li J, et al. Hydrogel formation upon photoinduced covalent capture of macrocycle stacks from dynamic combinatorial libraries. Angew Chem, Int Ed 2011;50: 8384–6.
- [26] Jin Y, et al. Malleable and recyclable thermosets: the next generation of plastics. Matter 2019;1(6):1456–93.
- [27] Adzima BJ, et al. Rheological and chemical analysis of reverse gelation in a covalently cross-linked Diels— Alder polymer network. Macromolecules 2008;41 (23):9112–7
- [28] Bowman CN, Kloxin CJ. Covalent adaptable networks: reversible bond structures incorporated in polymer networks. Angew Chem Int Ed 2012;51(18):4272–4.
- [29] Kloxin CJ, et al. Covalent adaptable networks (CANs): a unique paradigm in cross-linked polymers. Macromolecules 2010;43(6):2643–53.
- [30] Tasdelen MA. Diels-Alder "click" reactions: recent applications in polymer and material science. Polym Chem 2011;2(10):2133–45.
- [31] Wojtecki RJ, Meador MA, Rowan SJ. Using the dynamic bond to access macroscopically responsive structurally dynamic polymers. Nat Mater 2011;10(1):
- [32] Luo C, et al. Effects of bond exchange reactions and relaxation of polymer chains on the thermomechanical behaviors of covalent adaptable network polymers. Polymer 2018;153(26):43–51.
- [33] Park HY, et al. Stress relaxation by addition-fragmentation chain transfer in highly cross-linked thiol-yne networks. Macromolecules 2010;43(24):10188–90.
- [34] Hanzon D, et al. Creep-induced anisotropy in covalent adaptable network polymers. Soft Matter 2017. https://doi.org/10.1039/C7SM01174A.

- [35] Luo C, et al. Chemomechanics in the moisture-induced malleability of polyimine-based covalent adaptable networks. Macromolecules 2018;51(23):9825–38.
- [36] Luo C, et al. Chemomechanics of dual-stage reprocessable thermosets. J Mech Phys Solid 2019;126:168–86.
- [37] Yu K, et al. Reprocessing and recycling of thermosetting polymers based on bond exchange reactions. RSC Adv 2014;4(20):10108–17.
- [38] Yu K, et al. Influence of stoichiometry on the glass transition and bond exchange reactions in epoxy thermoset polymers. RSC Adv 2014;4:48682–90.
- [39] Hanzon D, et al. Adaptable liquid crystal elastomers with transesterification-based bond exchange reactions. Soft Matter 2018;14:951–60.
- [40] Zhang Y, Broekhuis AA, Picchioni F. Thermally self-healing polymeric materials: the next step to recycling thermoset polymers? Macromolecules 2009;42(6): 1906–12
- [41] Chen, X., et al., New thermally remendable highly cross-linked polymeric materials. Macromolecules. 36(6): p. 1802-1807.
- [42] Chen XX, et al. A thermally re-mendable cross-linked polymeric material. Science 2002;295(5560):1698–702.
- [43] He X, Hanzon DW, Yu K. Cyclic welding behavior of covalent adaptable network polymers. J Polym Sci B Polym Phys 2018;56(5):402–13.
- [44] Yu K, et al. Interfacial welding of dynamic covalent network polymers. J Mech Phys Solid 2016;94:1–17.
- [45] Yu K, et al. A computational model for surface welding in covalent adaptable networks using finite element analysis. J Appl Mech 2016;83(9):091002.
- [46] Johnson LM, et al. Controlled degradation of disulfide-based epoxy thermosets for extreme environments. Polymer 2015;64:84–92.
- [47] Luzuriaga ARd, et al. Epoxy resin with exchangeable disulfide crosslinks to obtain reprocessable, repairable and recyclable fiber-reinforced thermoset composites. Mater. Horiz. 2016;3:241–7.
- [48] Taynton P, et al. Repairable woven carbon fiber composites with full recyclability enabled by malleable polyimine networks. Adv Mater 2016;28(15):2904–9.
- [49] He X, et al. Recyclable 3D printing of polyimine-based covalent adaptable network polymers. 3D Print Addit Manuf 2019;6(1):31–9.
- [50] Shi Q, et al. Recyclable 3D printing of vitrimer epoxy. Materials Horizons 2017;4 (4):598–607.
- [51] Yu K, et al. Carbon fiber reinforced thermoset composite with near 100% recyclability. Adv Funct Mater 2016;26(33):6098–106.
- [52] Shi x, et al. Primary recycling of anhydride-cured engineering epoxy using alcohol solvent. Polym Eng Sci 2018;59(S2):E111–9.
- [53] Yu K, et al. Carbon fiber reinforced thermoset composite with near 100% recyclability. Adv Funct Mater 2016;26(33):6098–106.
- [54] Shi X, et al. Primary recycling of anhydride-cured engineering epoxy using alcohol solvent. Polym Eng Sci 2019;59(s2):E111–9.
- [55] Shi X, et al. A multiscale chemomechanics theory for the solvent-assisted recycling of covalent adaptable network polymers. J Mech Phys Solid 2020:103918.
- [56] Yu K, et al. Dissolution of covalent adaptable network polymers in organic solvent. J Mech Phys Solid 2017;109:78–94.
- [57] Taynton P, et al. Heat-or water-driven malleability in a highly recyclable covalent network polymer. Adv Mater 2014;26(23):3938–42.
- [58] Kuang X, et al. Recycling of epoxy thermoset and composites via good solvent assisted and small molecules participated exchange reactions. ACS Sustainable Chem Eng 2018;6(7):9189–97.
- [59] Kuang X, et al. Dissolution of epoxy thermosets via mild alcoholysis: the mechanism and kinetics study. RSC Adv 2018;8:1493–502.
- [60] Wang Q, et al. Mechanics of mechanochemically responsive elastomers. J Mech Phys Solid 2015;82:320–44.
- [61] Wiggins KM, Brantley JN, Bielawski CW. Polymer mechanochemistry: force enabled transformations. ACS Publications; 2012.
- [62] Ribas-Arino J, Marx D. Covalent mechanochemistry: theoretical concepts and computational tools with applications to molecular nanomechanics. Chem Rev 2012;112(10):5412–87.
- [63] Huang Z, Boulatov R. Chemomechanics: chemical kinetics for multiscale phenomena. Chem Soc Rev 2011;40(5):2359–84.
- [64] He X, Hanzon DW, Yu K. Cyclic welding behavior of covalent adaptable network polymers. J Polym Sci B Polym Phys 2018;56(5):402–13.
- [65] Yu K, et al. Interfacial welding of dynamic covalent network polymers. J Mech Phys Solid 2016;94:1–17.
- [66] Yu K, et al. A computational model for surface welding in covalent adaptable networks using finite-element analysis. J Appl Mech 2016;83(9).
- [67] Wang Q, Gao Z, Yu K. Interfacial self-healing of nanocomposite hydrogels: theory and experiment. J Mech Phys Solid 2017;109:288–306.